Supplementary section

Temperature induced MIT

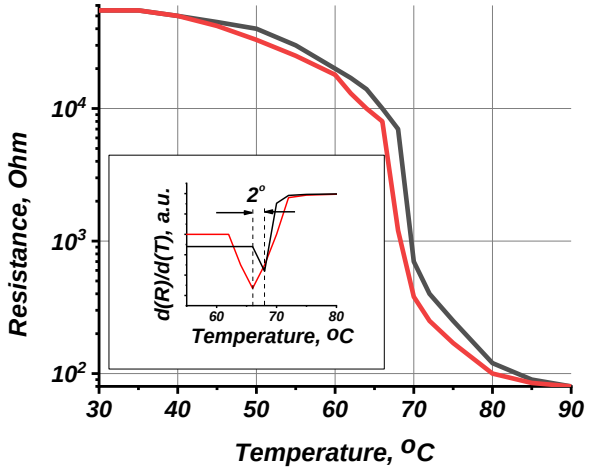

Figure S1. The electrical resistance plotted as a function of temperature for a VO_2 NC with an embedded conductive tip. The inset shows the first derivative of the R-T curve.

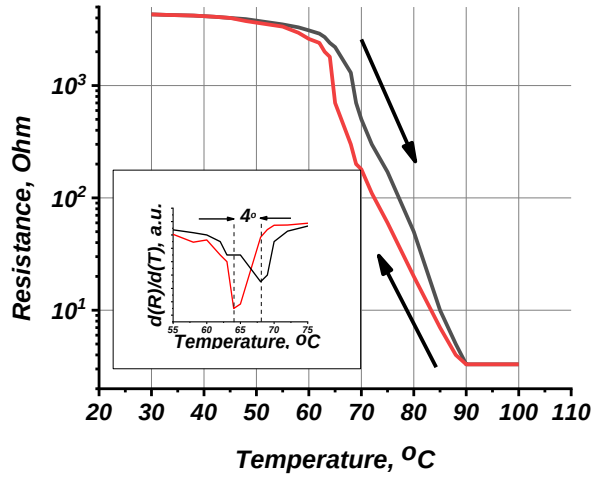

Figure S2. The electrical resistance plotted as a function of temperature for a VO_2 film. The inset shows the first derivative of the R-T curve.

A1. The distance from the tip to the surface of VO_2 NC

We estimated the minimum distance from the tip to the nearest crystal face of the NC. This quantity is an important one for evaluating the separation between the electrical contacts in the experiments with VO_2 NCs. To obtain this distance, we superimposed a TEM image of the tip after the synthesis of VO_2 onto an SEM image of the same tip before the synthesis (see Fig. S3). Indeed, the edges of the metal tip are distinctly seen on the TEM image. In the superimposing of the images, we used those edges for reference purposes. The distances from the tip to the nearest possible contact points of the VO_2 NC with the second contact (on the two upper crystal faces of the NC) were evaluated. These distances proved to be equal to 130 and 160 nm (with accuracy ±30 nm defined by the accuracy in superimposing the images). In the present article, in all calculations we used the minimum separation between the contacts to VO_2 equal to 100 nm.

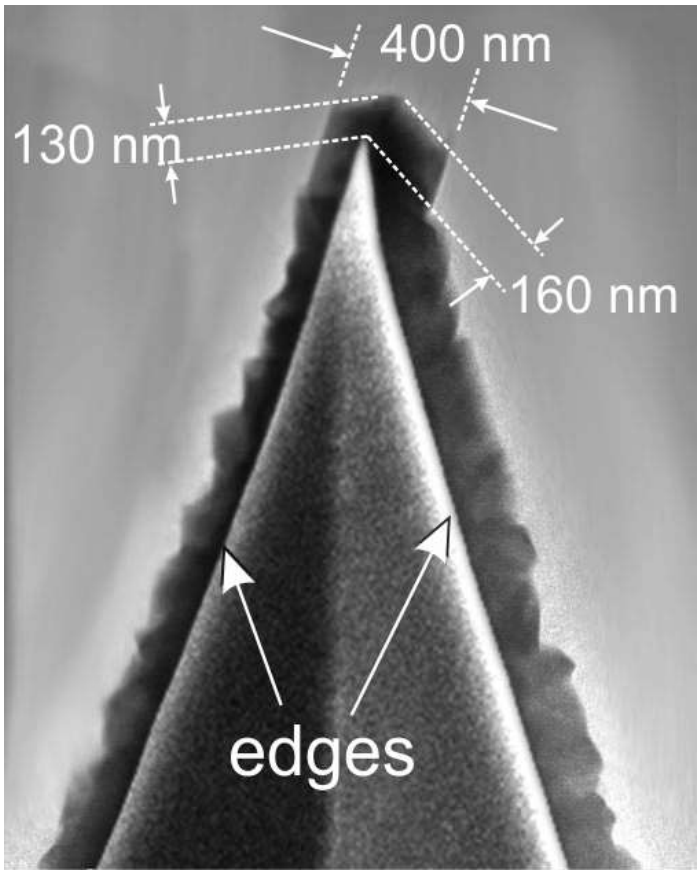

Figure S3. Superposition of an SEM image of one and the same tip onto its TEM image before and after the synthesis of VO_2 NCs on that tip. The distance from the tip to the nearest crystal face of the NC is 130±30 nm.

A2. Simple Joule heating model for VO_2 films and NCs

Fig. S4 a shows the temperature-dependent I-V characteristics of a VO_2 film grown on the flat surface of the holder chip. As it is seen from Fig. S4 a, when the external voltage was ramped up starting from zero, the current showed a linear increase. After the MIT occurred, on the attainment of the threshold voltage V_{MIT} the electric current jumped abruptly by several orders of magnitude. In the transient region, before the MIT occurred, a nonlinear behavior of the I-V curve is distinctly seen. This behavior can be indicative of either the Joule heating of the polycrystalline film and the related reduction of its resistance or an increase in the concentration of charge carriers due to the Poole-Frenkel mechanism [1-3].

To comprehend the microscopic mechanisms relevant to the electrically-triggered switching in VO_2 films, we proceed by assuming that the Joule heating can be the main factor causing the MIT in VO_2 [4]. In this model, the heat generated by Joule heating equals the heat loss via the thermal conduction to the surroundings[4]. The relation between the threshold voltage for MIT (V_{MIT}) and the ambient temperature (T_A) is

$$\frac{V_{MIT}^2}{R} = K_{eff}(T_C - T_A). \qquad (1)$$

In formula (1), K_{eff} is the effective thermal conductance of the VO_2 material and T_c is the crystal temperature. Providing that the squared threshold voltage for MIT V^2_{MIT} linearly depends on T_A, the Joule heating model well explains the MIT for the film.

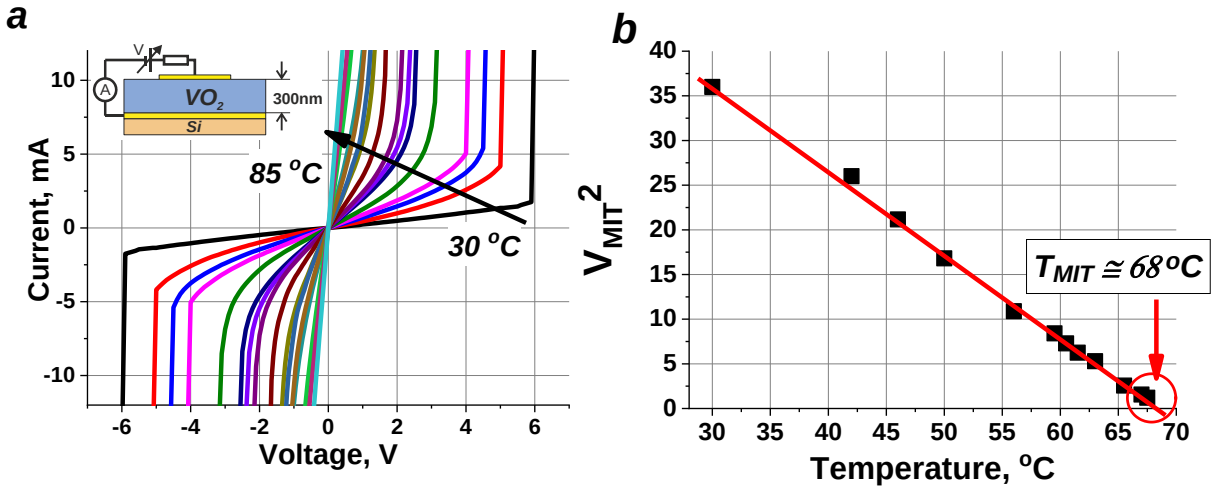

Figure S4. (a) Temperature-dependent I-V curves measured in vertical configuration and showing a sharp reversible MIT in a 300-nm thick VO_2 film grown on CoCr coating. The measurements were performed within the range of bias voltages ±6 V. The inset shows a schematic illustrating the sample geometry used for implementation of the electrically-triggered MIT. (b) A plot of V_{MIT}^2 versus T, where V_{MIT} is the voltage (in Volts) across the film right before MIT.

The curve of V^2_{MIT} *versus* T_C is shown in Fig. S4 b. According to equation (1), the linearity of the fitting dependence in Fig. S4 b confirms the fact that, here, the Joule heating model is appropriate for explaining the electrically-triggered MIT in the VO_2 film. Extrapolation of the fitting curve to the temperature axis gives for the transition point a temperature T_{MIT}=68 ^oC, this value being in good agreement with the temperature obtained from the temperature dependence of resistance at the phase transition. The least-square fitting provides the value of the slope, which proved to be equal to 0.92 V^2/K. Using the resistance value $R=1\div4\cdot10^3$ Ohm (obtained for a series of samples), one can estimate the effective thermal conductivity K_{eff}. The estimated value of K_{eff} falls into the range of 2.3 to $9.2\cdot10^{-4}$ W/K, which result well agrees with the data obtained in [4, 5].

Then, in order to analyze the influence of electric field on the electrically-triggered MIT, the critical electric fields $E_{MIT}=V_{MIT}/d$ (d is the thickness of the VO_2 film) right before the MIT were calculated. The magnitude of the estimated electric field at 30 ^oC proved to be 20 V/μm. Extrapolation of the fitting curve of Fig. S4 b to the temperature of 20 ^oC has yielded for the electric field a value of 22.4 V/μm; the latter value is much lower than the minimum value of the threshold electric field for MIT predicted by the electric-field-induced breakdown model[6]. Hence, our results suggest that the MIT in VO_2 films measured in the vertical configuration with flat contacts occurs due to the Joule heating rather than due to the field-induced breakdown effect.

Now, let us compare the dependence of squared threshold voltage V^2_{MIT} on temperature with formula (1). In Fig. S5, the points of V^2_{MIT} versus T_C are plotted. Evidently, the points in the graph do not fall onto a straight line. The latter means that the simple Joule heating model fails to provide an adequate explanation to the electrically-triggered phase transition in the VO_2 NC. Of course, for a detailed analysis of Joule heating as the main mechanism of MIT in a crystal, a more accurate model for such 3D nanostructures has to be developed taking into account all boundary conditions. However, this issue falls beyond the scope of this paper.

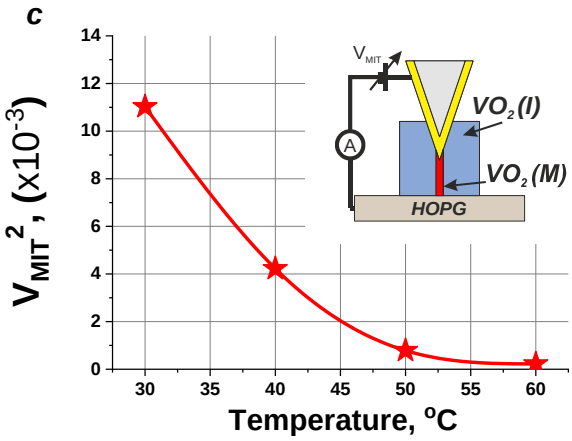

Figure S5. A plot of V_{MIT}^2 versus T, where V_{MIT} is the voltage across the NC right before MIT. The solid line is the guide to the eye. The inset shows a schematic that illustrates the emergence of a narrow current filament (red band) in the metallic VO_2(M) formed in the bulk of the insulating VO_2(I) on the attainment of the threshold voltage value.

Energy band diagram for CoCr-VO_2- HOPG interfaces

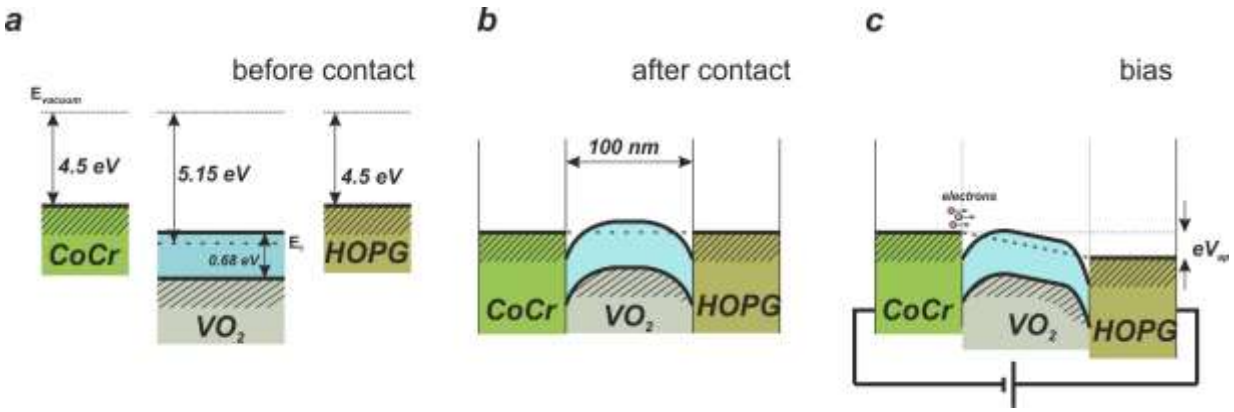

Figure S6. The band diagram of CoCr-VO_2-HOPG interfaces (schematically). The picture may be somewhat complicated if a tunnel-transparent thin oxide is present on the CoCr metal. a) The band diagram of the system before the materials are brought in contact. b) The same diagram after the contact is established at zero bias. The work functions of CoCr and HOPG are 4.5 eV, which value is noticeably lower than the work function of VO_2 (5.15 eV). When the materials are brought in contact, electrons are driven to flow from CoCr and HOPG to VO_2 until the Fermi levels of these materials, $E_F(VO_2)$, E_F(CoCr) and E_F(HOPG) become aligned. The bending of the VO_2 bands in the near-contact region is Φ_{VO2}-Φ_{Me}. c) The band diagram of the system biased with voltage V_{ap}. Electrons from the CoCr tip apex are transported via VO_2 to HOPG.

A3. The endurance test of VO_2 NCs using the application of voltage pulses

We carried out an endurance test of our VO_2 NCs using the pulse measurement circuit similar to that considered in the article (see Fig. S7). During one cycle, two pulses 25 ns wide were supplied to the sample, with the time interval between the pulses equal to 25 ns. The first pulse had amplitude above the threshold value of MIT (120 mV); this pulse conveyed the sample into high-conducting state. The second pulse had amplitude below the threshold value (90 mV); following this pulse, the sample remained in low-conducting state. The nanoswitch had operated more than 2×10^{11} times, and the test was terminated because its duration was too long. Two values of the electric current through the NC, the lower one under the supply of a 90-mV

amplitude testing pulse, and the upper one, under the supply of a 120-mV amplitude switching pulse, are shown in Fig. S7. The jump of the current is due to the formation of the nanosized current filament. The high stability of the pre- and post-MIT current values is due to the monocrystalline structure of the VO_2 NC and due to the small sizes of the VO_2 NCs.

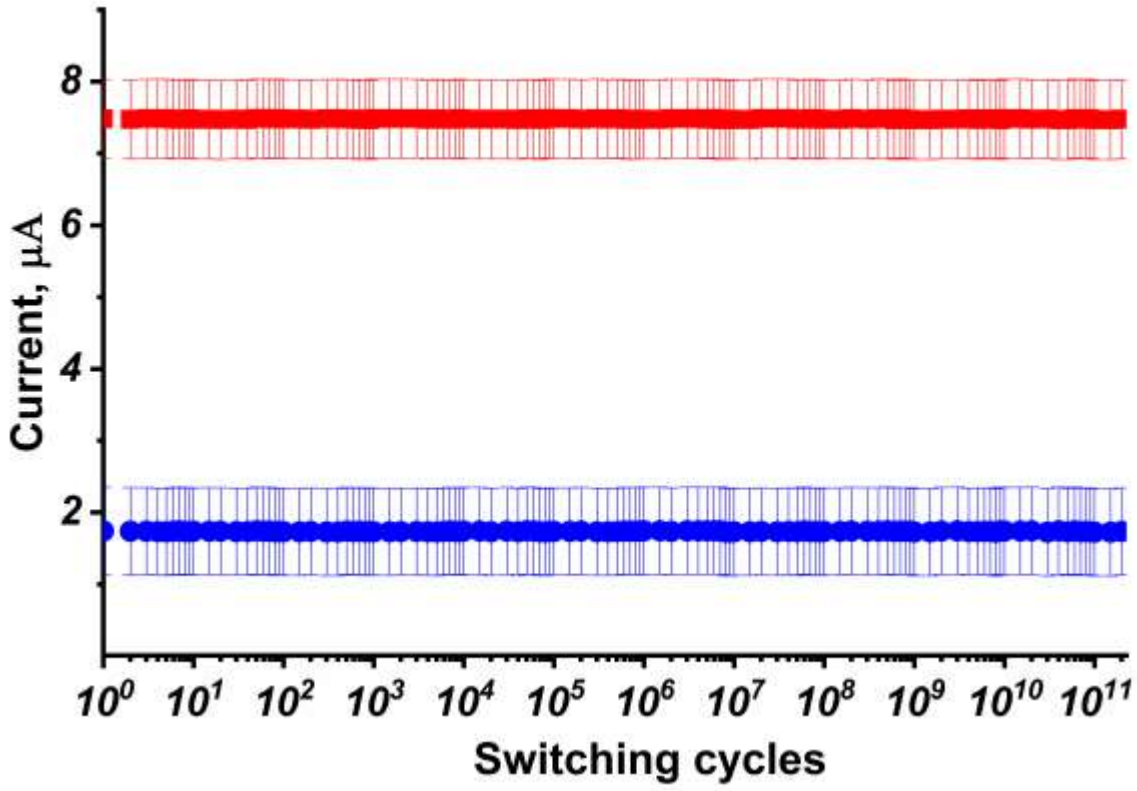

Figure S7. The endurance test of the VO_2 NC with an embedded sharp tip involving $2x10^{11}$ switching cycles. The error bars show the accuracy in evaluating the current values in our pulse measurements; this accuracy was defined by the ringing phenomenon.

References

1. Z. Yang, C. H. Ko, V. Balakrishnan, G. Gopalakrishnan and S. Ramanathan, *Phys Rev B*, 2010, **82**.
2. A. Beaumont, J. Leroy, J. C. Orlianges and A. Crunteanu, *J Appl Phys*, 2014, **115**.
3. D. Ruzmetov, G. Gopalakrishnan, J. D. Deng, V. Narayanamurti and S. Ramanathan, *J Appl Phys*, 2009, **106**.
4. B. S. Mun, J. Yoon, S. K. Mo, K. Chen, N. Tamura, C. Dejoie, M. Kunz, Z. Liu, C. Park, K. Moon and H. Ju, *Applied Physics Letters*, 2013, **103**.
5. J. Yoon, G. Lee, C. Park, B. S. Mun and H. Ju, *Applied Physics Letters*, 2014, **105**.
6. S. Hormoz and S. Ramanathan, *Solid State Electron*, 2010, **54**, 654-659.